

Supporting information

CsBO(OH)₂: a New Hydroxyborate with the Rare [BO(OH)₂] Group and deep ultraviolet cutoff edge

Jinbin Fan,[‡] Luyong Zhang,[‡] Zilong Chen, Huimin Li, Zhihua Yang, Yun Yang, Fangfang Zhang,^{*} and Shilie Pan^{*}

CONTENTS

Experimental Section

Table S1 Crystal data and structure refinement for CsBO(OH)₂.

Table S2 Inorganic borate compounds containing the isolated [BO_{3-x}(OH)_x] (x = 1, 2, 3) groups and their fundamental building blocks (FBBs). Structure data derived from the inorganic crystal structure database (ICSD) with version 5.3.0, the latest release of ICSD-2024/02.

Table S3 Selected bond lengths (Å) and angles (°) for CsBO(OH)₂.

Table S4 Atomic coordinates ($\times 10^4$), equivalent isotropic displacement parameters ($\text{\AA}^2 \times 10^3$), and bond valence sum (BVS) calculations for CsBO(OH)₂.

Table S5 Anisotropic displacement parameters ($\text{\AA}^2 \times 10^3$) for CsBO(OH)₂.

Table S6 Hydrogen atom coordinates ($\text{\AA} \times 10^4$) and isotropic displacement parameters ($\text{\AA}^2 \times 10^3$) for CsBO(OH)₂.

Table S7 Hydrogen bonds for CsBO(OH)₂. D, donor; H, hydrogen; A, acceptor.

Fig. S1 Statistics of compounds containing isolated [BO_{3-x}(OH)_x] (x = 1, 2, 3) groups. Structure data derived from the ICSD with version 5.3.0, the latest release of ICSD-2024/02.

Fig. S2 (a) A pair of [BO₃] in Cs₃BO₃. (b) The structure of Cs₃BO₃. (c) The structure of CsBO(OH)₂. (d) A pair of [BO(OH)₂] formed after hydroxylation of [BO₃] in CsBO(OH)₂.

Fig. S3 Comparison of the arrangement angles between adjacent [BO₃] groups in CsBO(OH)₂ and Cs₃BO₃.

Fig. S4 The TG and DSC curves of CsBO(OH)₂.

Fig. S5 The electronic structure of CsBO(OH)₂.

Fig. S6 The electronic structure of Cs₃BO₃.

Fig. S7 The total and partial density of states of CsBO(OH)₂.

Fig. S8 The calculated birefringence of Cs₃BO₃.

Experimental Section

Materials

CsOH·H₂O (95 %) and HBO₂ (99 %) were purchased from Aladdin and used as received.

Single-Crystal Growth

Single crystals of CsBO(OH)₂ were obtained by a hydrothermal method. CsOH·H₂O (1.19 g, 7.1 mmol) was mixed with HBO₂ (0.31g, 7.1 mmol) in a 23 mL Teflon-lined stainless-steel autoclave. The autoclave was sealed and rapidly heated to 220 °C and held at this temperature for 133 h, then slowly cooled to 180 °C at 1.7 °C·h⁻¹, then to 110 °C at 3.4 °C·h⁻¹, followed by rapid cooling to room temperature. Centimeter-sized single crystals were obtained.

Single-Crystal X-ray Diffraction (XRD)

The single-crystal XRD data of CsBO(OH)₂ were collected using a Bruker D8 Venture X-ray single-crystal diffractometer, equipped with a PHOTON III C28 detector and utilizing graphite-monochromated Mo K α radiation ($\lambda = 0.71073 \text{ \AA}$). Data collection and integration were carried out with the SAINT-Plus program.¹ The positions of heavy atoms in the structure were determined via the direct method, while the positions of light atoms were refined through differential Fourier synthesis within the SHELXTL system.² The single-crystal data were processed using Olex2.³ The final refinement of atomic coordinates and anisotropic thermal parameters was performed using full-matrix least-squares methods based on F_0^2 with data having $F_0^2 \geq 2\sigma(F_0^2)$ until convergence was achieved. To validate the structure, potential missing symmetry elements were examined using PLATON.⁴ The structure file in CIF format was also checked for consistency and integrity using IUCrcheckCIF (<http://checkcif.iucr.org>).

Powder X-ray diffraction (PXRD)

PXRD measurements were conducted using a Bruker D2 Phaser X-ray diffractometer with graphite monochromated Cu K α radiation ($\lambda = 1.5418 \text{ \AA}$). Diffraction data were collected at room temperature, with 2 θ angles ranging from 5 to 70 °, a step width of 0.02 °, and a fixed counting time of 1 second per step.

Infrared (IR) Spectroscopy

The IR spectrum of CsBO(OH)₂ was recorded using a Shimadzu IR Affinity-1 Fourier transform infrared spectrometer, covering the range from 400 to 4000 cm⁻¹ at

room temperature, with a resolution of 1 cm^{-1} . The sample was mixed with KBr at a 1:100 ratio, ground thoroughly, and then pressed into a pellet. It was subsequently dried under an infrared lamp before testing.

Thermal Analysis

The thermal gravimetric (TG) and differential scanning calorimetry (DSC) analyses of CsBO(OH)_2 were performed using a NETZSCH STA 449 F3 thermal analyzer, under a N_2 flow atmosphere. The sample was heated from 40 to $800\text{ }^\circ\text{C}$ at a rate of $10\text{ }^\circ\text{C}\cdot\text{min}^{-1}$ in a crucible.

Transmittance Spectroscopy

The transmittance spectrum of a crystal plate, was recorded in the range of 175 - 1500 nm at room temperature using a Shimadzu Solid Spec-3700 DUV spectrophotometer to determine the cutoff edge of CsBO(OH)_2 crystal.

Microscopic Measurement of Birefringence

The single crystal was tested for birefringence using a cross-polarizing microscope. A strip of single crystal with a measured thickness was selected for preliminary birefringence assessment, performed on a ZEISS Axio Scope.5 microscope equipped with a quartz wedge compensator, under a 546 nm light source. The birefringence was calculated using the following equation:

$$R = |N_g - N_p| \times d = \Delta n \times d$$

N_g , N_p , and Δn represent the refractive indices of fast light, slow light, and the birefringence, respectively. R represents the optical path difference, while d refers to the crystal thickness. It is important to note that the crystal orientation was not considered in the above method for the biaxial crystal. Therefore, the actual birefringence of the crystal is greater than or equal to the measured value.

Theoretical Calculation

First-principles calculations were performed to investigate the relationship between the electronic structure and optical properties using the plane-wave pseudopotential method based on DFT,⁵ as implemented in the CASTEP package⁶. The generalized gradient approximation (GGA) with the Perdew-Burke-Ernzerhof (PBE) functional and norm-conserving pseudopotentials (NCP) was employed to describe the exchange-correlation functional and pseudopotentials.⁷ To ensure convergence of the calculation results, a plane-wave basis set cutoff energy of 750 eV and was employed. The Brillouin zone numerical integration was implemented by using $4 \times 4 \times 3(\text{CsBO(OH)}_2)$ and $3 \times 3 \times 3(\text{Cs}_3\text{BO}_3)$ Monkhorst-Pack k -point

parameters.⁸ Other calculation parameters and convergence criteria were set to the default values in the CASTEP code.

Generally, the band gap tends to be underestimated due to the limited accuracy of the exchange-correlation energy within the GGA method. Therefore, a scissors operator was applied to correct for this discrepancy, defined as the difference between the experimental and calculated GGA band gaps for CsBO(OH)₂. The HSE06 was adopted to afford more precise band gap values.

The linear optical properties were examined based on the dielectric function $\varepsilon(\omega) = \varepsilon_1(\omega) + i\varepsilon_2(\omega)$.⁹ The imaginary part of the dielectric function (ε_2) can be calculated from the electronic structures, while the real part is obtained through the Kramers-Kronig transformation. Consequently, the refractive indices and birefringence can be derived.

Table S1 Crystal data and structure refinement for CsBO(OH)₂.

Empirical formula	CsBO(OH) ₂
Temperature (K)	298.00
Crystal system, Space group	Monoclinic, <i>P2₁/n</i>
<i>a</i> (Å), α (°)	7.5268(4), 90
<i>b</i> (Å), β (°)	6.9794(4), 113.612(2)
<i>c</i> (Å), γ (°)	7.8192(4), 90
Volume (Å ³)	376.37(4)
<i>Z</i> , Calculated density (g·cm ⁻³)	4, 3.419
Absorption coefficient (mm ⁻¹)	9.656
<i>F</i> (000)	344
2Theta range for data collection (°)	6.35 to 54.948
Limiting indices	$-9 \leq h \leq 9, -9 \leq k \leq 9, -10 \leq l \leq 10$
Reflections collected / unique	6485 / 864 [R(int) = 0.0393]
Completeness to theta	100 %
Data / restraints / parameters	864 / 0 / 55
Goodness-of-fit on <i>F</i> ²	1.088
Final <i>R</i> indices [$F_o^2 > 2\sigma(F_o^2)$] ^a	$R_1 = 0.0159, wR_2 = 0.0370$
<i>R</i> indices (all data) ^a	$R_1 = 0.0187, wR_2 = 0.0378$
Largest diff. peak and hole (e·Å ⁻³)	0.50 and -0.64

^a $R_1 = \sum ||F_o| - |F_c|| / \sum |F_o|$ and $wR_2 = [\sum_w (F_o^2 - F_c^2)^2 / \sum_w F_o^4]^{1/2}$ for $F_o^2 > 2\sigma(F_o^2)$.

Table S2 Inorganic borate compounds containing the isolated [BO_{3-x}(OH)_x] (x = 1, 2, 3) groups and their fundamental building blocks (FBBs). Structure data derived from the inorganic crystal structure database (ICSD) with version 5.3.0, the latest release of ICSD-2024/02.

Compounds	Space groups	FBBs	Ref.
[BO ₂ (OH)]			
Na ₂ [BO ₂ (OH)]	<i>Pnma</i>		10
Na ₂ [BO ₂ (OH)]·H ₂ O	<i>Pca2₁</i>		11
BaBO ₂ (OH)	<i>P2₁2₁2₁</i>	[BO ₂ (OH)]	12
Pb ₂ O[BO ₂ (OH)]	<i>C2/m</i>		13

$\text{Pb}_2[\text{BO}_2(\text{OH})](\text{SO}_4)$	$P2_1/m$	14
$\text{CaBO}_2(\text{OH})$	$P2_1/c$	15
$\text{SrBO}_2(\text{OH})$	$Pnma$	16
$\text{Bi}_2\text{O}_2[\text{BO}_2(\text{OH})]$	Cm	17
$\text{Sr}_5[\text{BO}_2(\text{OH})]_3(\text{OH})_3\text{F}$	$P2_1/m$	18
$\text{Na}(\text{Na}_{0.998}\text{Ce}_{0.01})(\text{Ce}_{1.994})(\text{BO}_2(\text{OH}))(\text{BO}_3)_2 \cdot (\text{H}_2\text{O})$	$C2mm$	19
$[\text{BO}(\text{OH})_2]$		
$\text{Cu}_2[\text{BO}(\text{OH})_2](\text{OH})_3$	$Pnma$	$[\text{BO}(\text{OH})_2]$ 20
$[\text{B}(\text{OH})_3]$		
$\text{KF} \cdot \text{B}(\text{OH})_3$	$Pbcm$	21
$\text{Cs}_3[\text{B}(\text{OH})_3]_2\text{Cl}_3$	$C2/c$	22
$\text{Cs}[\text{B}(\text{OH})_3][\text{B}_3\text{O}_3(\text{OH})_3]\text{Cl}$	$P2_1/c$	22
$\text{Rb}_3[\text{B}(\text{OH})_3][\text{B}_3\text{O}_3(\text{OH})_3]_2\text{Cl}_3$	$P6_3/m$	22
H_3BO_3	$P\bar{1}$	23
$\text{PbxBa}_{3-x}(\text{OH})(\text{B}_9\text{O}_{16}) \cdot \text{B}(\text{OH})_3$ ($x = 0, 0.84, 1.5$ and 3)	$P31c$	24
$\text{Ba}_3\text{Na}_{0.9}(\text{OH})_{1.9}[\text{B}_9\text{O}_{16}][\text{B}(\text{OH})_3]$	$P31c$	25
$\text{Ba}_2[\text{B}_5\text{O}_8(\text{OH})]_2[\text{B}(\text{OH})_3] \cdot \text{H}_2\text{O}$	$P2_1$	26
$\text{Ca}_2[\text{B}_5\text{O}_8(\text{OH})]_2[\text{B}(\text{OH})_3] \cdot \text{H}_2\text{O}$	Cc	27
$\beta\text{-Ca}_2(\text{B}_5\text{O}_8\text{OH})_2[\text{B}(\text{OH})_3] \cdot \text{H}_2\text{O}$	$P1$	$[\text{B}(\text{OH})_3]$ 28
$\text{Sr}_2[\text{B}_5\text{O}_8(\text{OH})]_2[\text{B}(\text{OH})_3] \cdot \text{H}_2\text{O}$	$P1$	29
$\text{Ca}[\text{B}_5\text{O}_8(\text{OH})][\text{B}(\text{OH})_3] \cdot 3\text{H}_2\text{O}$	$P2_1/a$	30
$\text{NaB}_6\text{O}_8(\text{OH})_3\text{B}(\text{OH})_3 \cdot 6\text{H}_2\text{O}$	$P2_1/c$	31
$\text{SmB}_6\text{O}_8(\text{OH})_5\text{B}(\text{OH})_3$	$P\bar{1}$	32
$\text{Eu}[\text{B}_6\text{O}_8(\text{OH})_5] \cdot \text{H}_3\text{BO}_3$	$P\bar{1}$	33
$\text{SmB}_6\text{O}_8(\text{OH})_5\text{B}(\text{OH})_3 \cdot \text{H}_2\text{O}$	$C2/m$	32
$\text{Ba}_6[\text{B}_6\text{O}_9(\text{OH})_6]_2\text{B}(\text{OH})_3$	$R\bar{3}$	34
$\text{Na}_5\text{Ga}[\text{B}_7\text{O}_{12}(\text{OH})]_2 \cdot 2\text{B}(\text{OH})_3$	$C2$	35
$\text{K}_7\text{Ni}[\text{B}_{18}\text{O}_{24}(\text{OH})_9](\text{NO}_3)_6 \cdot (\text{H}_3\text{BO}_3)$	$R\bar{3}$	36
$\text{Na}_2[\text{B}_8\text{O}_{11}(\text{OH})_4] \cdot \text{B}(\text{OH})_3 \cdot 2\text{H}_2\text{O}$	$P2_1/c$	37

Table S3. Selected bond lengths (Å) and angles (°) for CsBO(OH)₂.

B1-O1	1.392(4)	Cs1-O1 ^{#6}	3.531(2)
B1-O2	1.330(4)	Cs1-O2 ^{#3}	3.271(2)
B1-O3	1.384(4)	Cs1-O2	3.147(2)
Cs1-O1 ^{#3}	3.671(2)	Cs1-O3 ^{#1}	3.276(2)
Cs1-O1 ^{#5}	3.198(2)	Cs1-O3	3.207(2)
Cs1-O1 ^{#4}	3.194(2)	Cs1-O3 ^{#2}	3.261(2)
O2-B1-O1	122.6(3)	O2-Cs1-O1 ^{#4}	128.97(5)
O3-B1-O1	116.5(3)	O2 ^{#3} -Cs1-O1 ^{#4}	45.19(5)
O2-B1-O3	120.9(3)	O2 ^{#3} -Cs1-O3 ^{#2}	155.23(6)
O1 ^{#6} -Cs1-O1 ^{#3}	62.90(3)	O2-Cs1-O3	43.62(5)
O1 ^{#5} -Cs1-O1 ^{#4}	64.640(17)	O2-Cs1-O2 ^{#3}	99.24(5)
O1 ^{#5} -Cs1-O1 ^{#6}	101.22(5)	O2 ^{#3} -Cs1-O1 ^{#3}	39.70(5)
O1 ^{#6} -Cs1-O1 ^{#4}	95.85(6)	O2-Cs1-O1 ^{#3}	117.95(5)
O1 ^{#4} -Cs1-O1 ^{#3}	62.07(6)	O2-Cs1-O1 ^{#6}	131.41(6)
O1 ^{#5} -Cs1-O1 ^{#3}	121.42(7)	O3-Cs1-O3 ^{#1}	81.10(4)
O1 ^{#6} -Cs1-O2 ^{#3}	101.62(5)	O3 ^{#1} -Cs1-O3 ^{#2}	77.06(5)
O1 ^{#5} -Cs1-O2 ^{#3}	107.44(6)	O3 ^{#1} -Cs1-O2 ^{#3}	82.82(6)
O1 ^{#5} -Cs1-O3	85.19(5)	O3 ^{#1} -Cs1-O1 ^{#4}	127.97(5)
O1 ^{#6} -Cs1-O3 ^{#2}	65.42(5)	O3 ^{#2} -Cs1-O1 ^{#4}	150.97(5)
O1 ^{#5} -Cs1-O3 ^{#1}	160.57(5)	O3-Cs1-O1 ^{#3}	114.41(5)
O1 ^{#6} -Cs1-O3	173.55(6)	O3-Cs1-O3 ^{#2}	113.51(4)
O1 ^{#5} -Cs1-O3 ^{#2}	96.09(6)	O3-Cs1-O2 ^{#3}	76.88(5)
O1 ^{#6} -Cs1-O3 ^{#1}	92.51(5)	O3 ^{#2} -Cs1-O1 ^{#3}	120.13(5)
O2-Cs1-O3 ^{#1}	47.53(5)	O3 ^{#1} -Cs1-O1 ^{#3}	77.10(5)
O2-Cs1-O3 ^{#2}	77.64(5)	O3-Cs1-O1 ^{#4}	87.51(5)
O2-Cs1-O1 ^{#5}	113.49(5)		

Symmetry transformations used to generate equivalent atoms:

^{#1}1/2+X, 1/2-Y, 1/2+Z^{#2}1/2-X, 1/2+Y, 3/2-Z^{#3}1/2-X, Y-1/2, 3/2-Z^{#4}X-1/2, 1/2-Y, 1/2+Z^{#5}-X, 1-Y, 1-Z^{#6}X, Y, 1+Z^{#7}X-1/2, 1/2-Y, Z-1/2^{#8}1/2+X, 1/2-Y, Z-1/2^{#9}X, Y, Z-1

Table S4. Atomic coordinates ($\times 10^4$), equivalent isotropic displacement parameters ($\text{\AA}^2 \times 10^3$), and bond valence sum (BVS) calculations for CsBO(OH)_2 .

Atom	x	y	z	U_{eq}^{a}	BVS ^b
Cs1	1572.5(3)	3610.7(2)	8799.4(2)	29.73(10)	0.85
B1	2626(5)	3668(4)	4765(4)	23.0(6)	3.03
O1	2603(3)	4440(3)	3115(3)	31.8(5)	/
O2	4074(3)	3968(3)	6414(3)	34.5(5)	1.94
O3	1026(3)	2593(3)	4618(3)	30.6(5)	/

^a U_{eq} is defined as one third of the trace of the orthogonalized U_{ij} tensor.

^bBVS are calculated by using the bond-valence model ($S_i = \exp [(R_o - R_i) / b]$, where R_o (in angstroms) is an empirical constant with values 2.417 for Cs-O bonds and 1.371 for B-O bonds and, R_i is the length of bond i (in angstroms), and $b = 0.37 \text{ \AA}$).

Table S5. Anisotropic displacement parameters ($\text{\AA}^2 \times 10^3$) for CsBO(OH)_2

Atom	U_{11}	U_{22}	U_{33}	U_{23}	U_{13}	U_{12}
Cs1	29.49(14)	30.46(12)	31.61(14)	-1.40(6)	14.73(10)	0.32(6)
B1	23.3(16)	20.7(13)	24.9(16)	1.3(10)	9.4(13)	3.7(10)
O1	29.4(12)	39.5(11)	23.3(10)	5.3(8)	7.1(9)	-7.7(10)
O2	25.8(11)	48.7(12)	24.6(11)	7.7(8)	5.6(9)	-6.8(9)
O3	32.9(12)	36.5(11)	23.1(11)	-5.3(8)	12.2(10)	-11.3(8)

Table S6. Hydrogen atom coordinates ($\text{\AA} \times 10^4$) and isotropic displacement parameters ($\text{\AA}^2 \times 10^3$) for CsBO(OH)_2 .

Atom	x	y	z	U_{eq}
H1	3460(60)	4980(60)	3300(50)	51(12)
H3	420(50)	2330(50)	3650(40)	31(9)

Table S7. Hydrogen bonds for CsBO(OH)_2 . D, donor; H, hydrogen; A, acceptor.

D-H \cdots A	$d_{(\text{D-H})} (\text{\AA})$	$d_{(\text{H}\cdots\text{A})} (\text{\AA})$	$d_{(\text{D-A})} (\text{\AA})$	$\text{D-H-A} (\text{\AA})$
O1-H1 \cdots O2 ^{#1}	0.888(10)	1.712(14)	2.581(3)	166(4)

O3-H3 \cdots O3 ^{#2}	0.892(10)	1.737(13)	2.621(3)	171(4)
---------------------------------	-----------	-----------	----------	--------

Symmetry transformations used to generate equivalent atoms:

^{#1} X-1/2, 3/2-Y, Z-1/2 ^{#2} 1-X, 1-Y, 1-Z

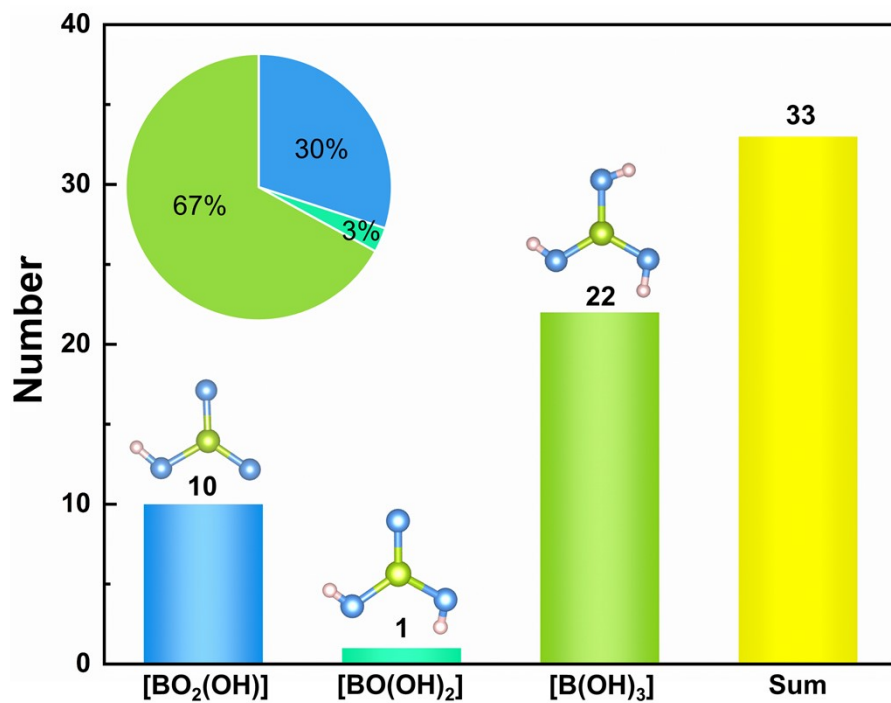


Fig. S1 Statistics of compounds containing isolated $[\text{BO}_{3-x}(\text{OH})_x]$ ($X = 1, 2, 3$) groups. Structure data derived from the ICSD with version 5.3.0, the latest release of ICSD-2024/02.

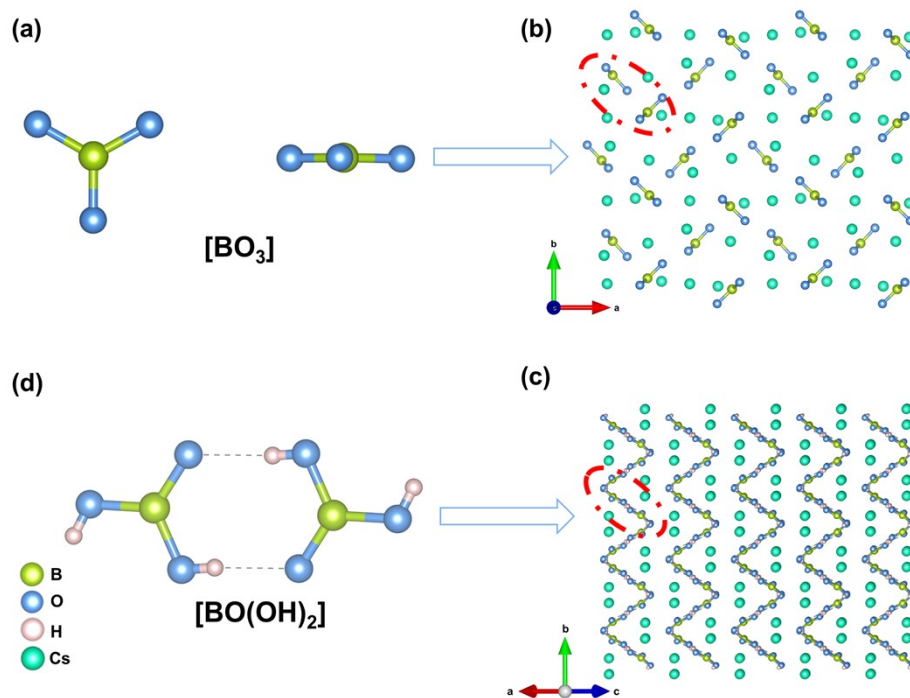


Fig. S2 (a) A pair of $[\text{BO}_3]$ in Cs_3BO_3 . (b) The structure of Cs_3BO_3 . (c) The structure of $\text{CsBO}(\text{OH})_2$. (d) A pair of $[\text{BO}(\text{OH})_2]$ formed after hydroxylation of $[\text{BO}_3]$ in $\text{CsBO}(\text{OH})_2$.

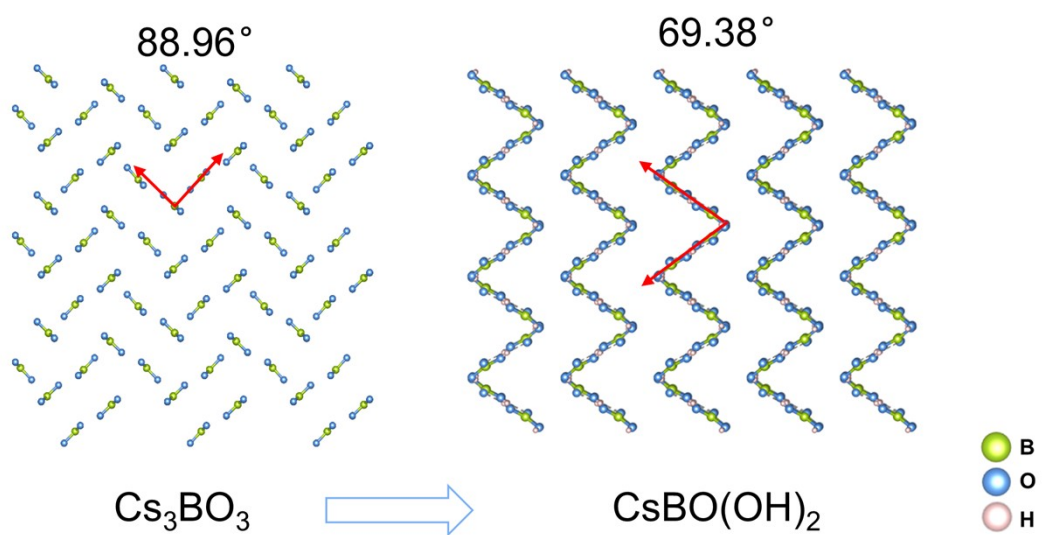


Fig. S3. Comparison of the arrangement angles between adjacent $[\text{BO}_3]$ groups in $\text{CsBO}(\text{OH})_2$ and Cs_3BO_3 .

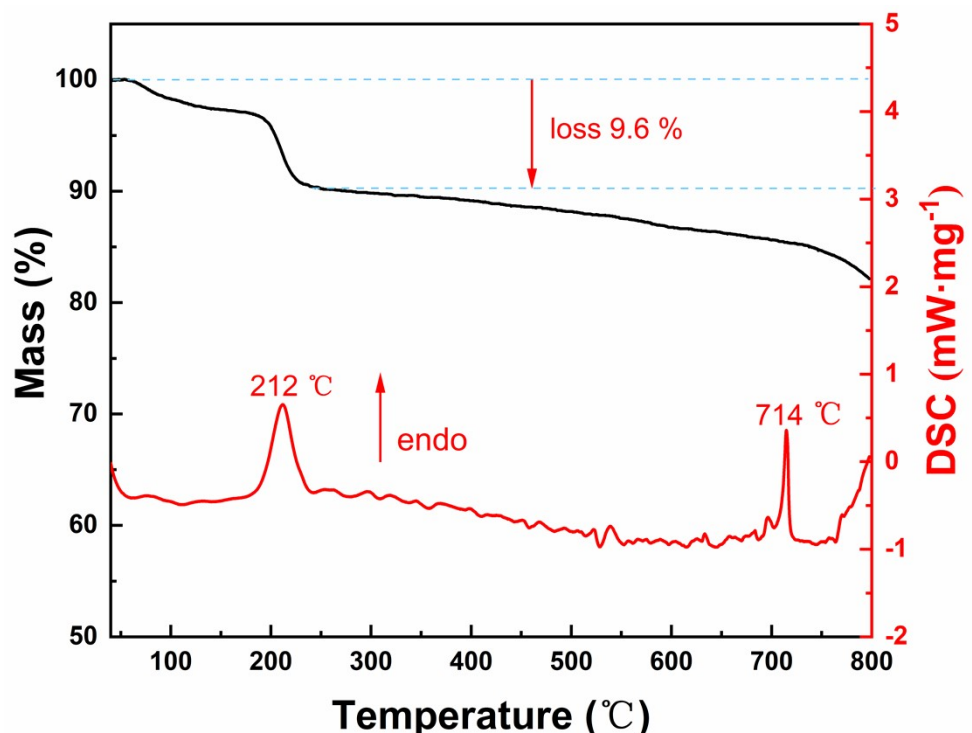


Fig. S4 The TG and DSC curves of $\text{CsBO}(\text{OH})_2$.

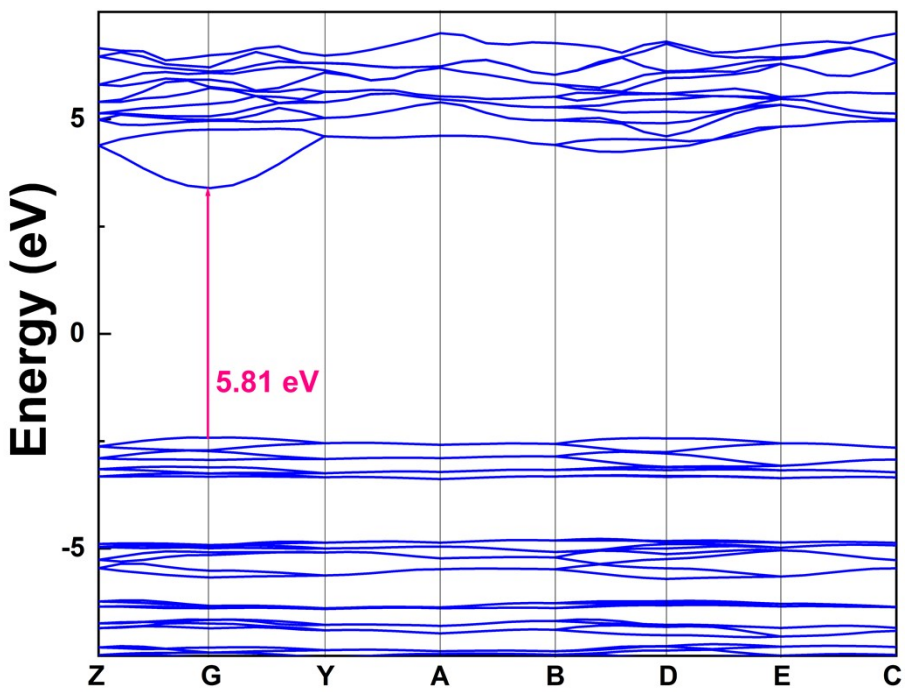


Fig. S5 The electronic structure of $\text{CsBO}(\text{OH})_2$.

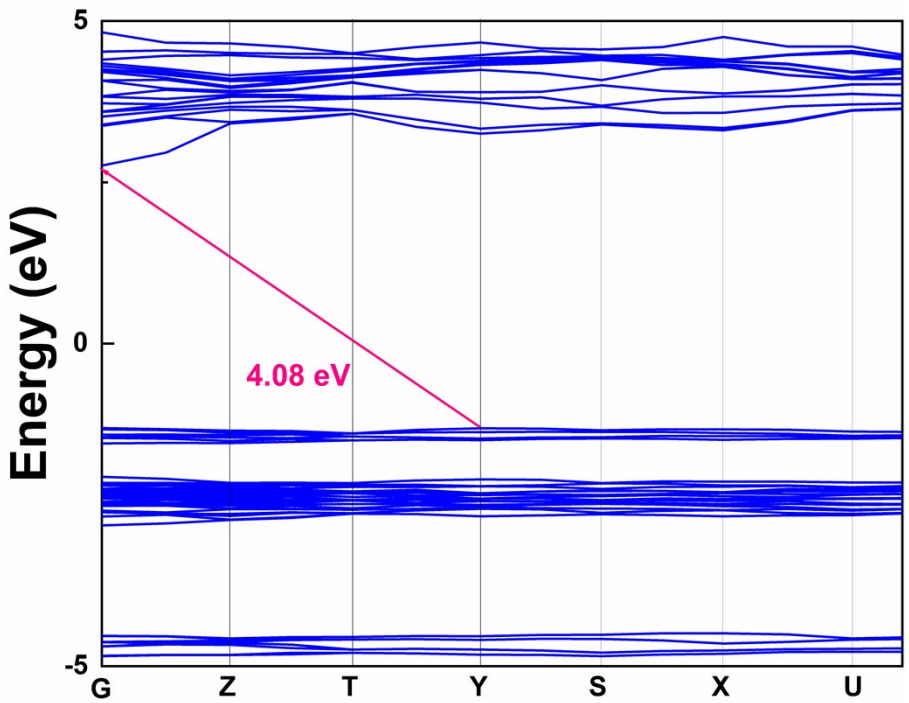


Fig. S6 The electronic structure of Cs_3BO_3 .

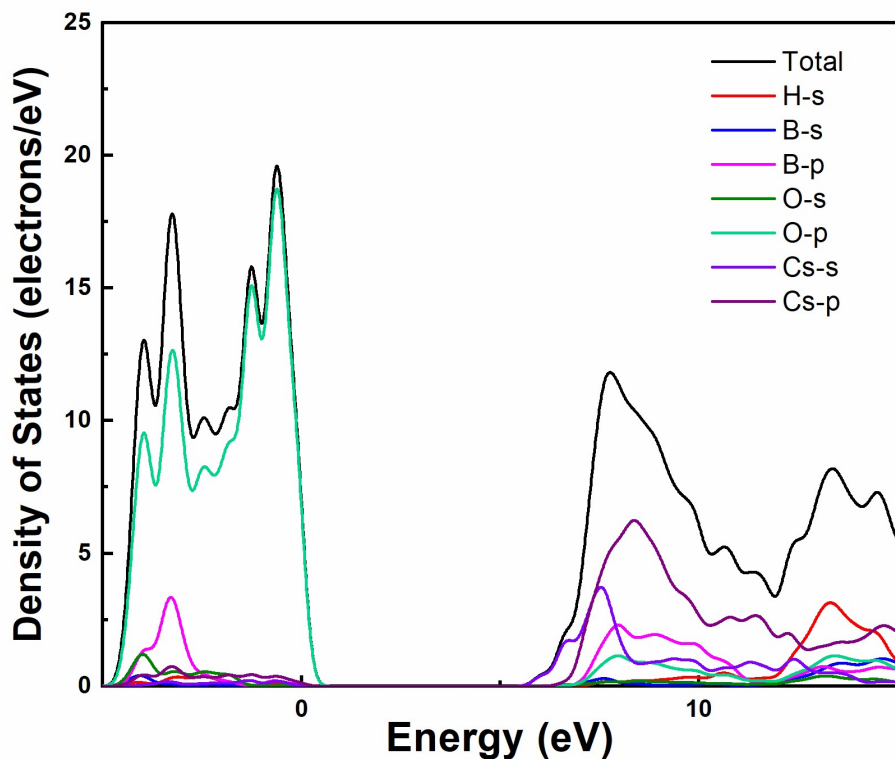


Fig. S7 The total and partial density of states of $\text{CsBO}(\text{OH})_2$.

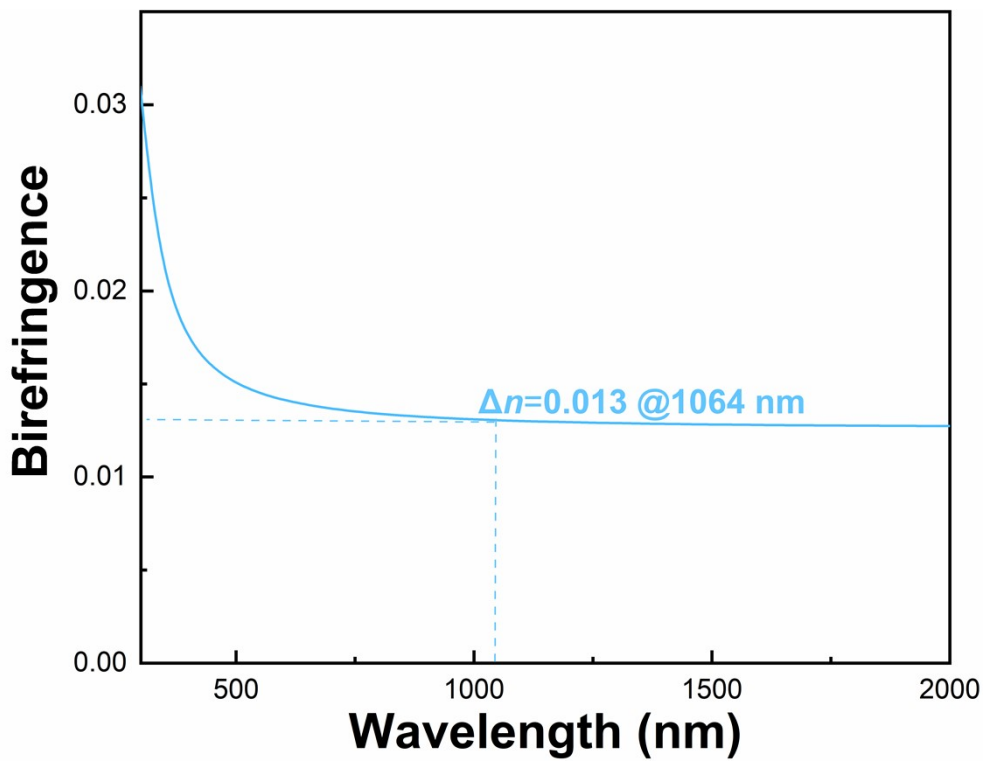


Fig. S8 The calculated birefringence of Cs_3BO_3 .

References

1. P J T i n c r f t r SAINT.
2. G M J A C A Sheldrick, 2015, **71**, 3-8.
3. O Dolomanov, L Bourhis, R Gildea and J Howard, *Journal.*
4. A J J o a c Spek, 2003, **36**, 7-13.
5. L J Sham and M Schlüter, *Phys. Rev. Lett.*, 1983, **51**, 1888-1891.
6. S J Clark, M D Segall, C J Pickard, P J Hasnip, M I J Probert, K Refson and M C Payne, 2005, **220**, 567-570.
7. J P Perdew, K Burke and M Ernzerhof, *Phys. Rev. Lett.*, 1996, **77**, 3865-3868; A M Rappe, K M Rabe, E Kaxiras and J D Joannopoulos, *Phys Rev B*, 1990, **41**, 1227-1230.
8. H J Monkhorst and J D Pack, *Phys Rev B*, 1976, **13**, 5188-5192.
9. J E Sipe and E Ghahramani, *Phys Rev B*, 1993, **48**, 11705-11722.
10. S Menchetti and C Sabelli, *Acta Crystallographica Section B*, 1982, **38**, 1282-1285.
11. W Zhao, *J. Mol. Struct.*, 2017, **1127**, 252-256.
12. Y Li, P A Hegarty, M Rüsing, L M Eng and M Ruck, *Z. Anorg. Allg. Chem.*, 2022, **648**, e202200193.
13. F Sun, L Wang and C C Stoumpos, *J. Solid State Chem.*, 2016, **240**, 61-66.
14. T-T Ruan, W-W Wang, C-L Hu, X Xu and J-G Mao, *J. Solid State Chem.*, 2018, **260**, 39-45.
15. W Sun, Y-X Huang, Z Li, Y Pan and J-X Mi, *The Canadian Mineralogist*, 2011, **49**, 823-834.
16. Z-T Yu, Z Shi, W Chen, Y-S Jiang, H-M Yuan and J-S Chen, *J. Chem. Soc., Dalton Trans.*, 2002, DOI: 10.1039/B110468C, 2031-2035.
17. R Cong, J Sun, T Yang, M Li, F Liao, Y Wang and J Lin, *Inorg. Chem.*, 2011, **50**, 5098-5104.
18. Y Dong, L Gao and Z Su, *J. Mol. Struct.*, 2021, **1227**, 128915.
19. A P Topnikova, E L Belokoneva, O V Dimitrova and A S Volkov, *Crystallography Reports*, 2016, **61**, 940-944.
20. A A Vorobyova, A I Shilov, F M Spiridonov, A V Knotko, I L Danilovich, A N Vasiliev and I V Morozov, *Russ. Chem. Bull.*, 2020, **69**, 704-711.
21. Y Li, X Chen and K M Ok, *Chem. Commun.*, 2022, **58**, 8770-8773.
22. J Jiao, M Cheng, R Yang, Y Yan, M Zhang, F Zhang, Z Yang and S Pan, *Angew. Chem. Int. Ed.*, 2022, **61**, e202205060.
23. W H Zachariasen, *Acta Crystallogr*, 1954, **7**, 305-310.
24. J Lu, G Shi, H Wu, M Wen, D Hou, Z Yang, F Zhang and S J R a Pan, 2017, **7**, 20259-20265; E L Belokoneva, S Y Stefanovich, O V Dimitrova, N N Mochanova and N V Zubkova, *Crystallography Reports*, 2009, **54**, 814-821.
25. A P Topnikova, E L Belokoneva, O V Dimitrova, A S Volkov and L V Zorina, *Crystallography Reports*, 2023, **68**, 237-241.
26. H-Q Wu and Y-Y Li, *Inorg. Chem. Commun.*, 2020, **121**, 108220.
27. Q Wei, J-W Cheng, C He and G-Y Yang, *Inorg. Chem.*, 2014, **53**, 11757-11763.

28. Q-M Qiu, X-Y Li, C-A Chen, K-N Sun and G-Y Yang, *J. Solid State Chem.*, 2021, **299**, 122193.
29. W-F Chen, J-Y Lu, J-J Li, Y-Z Lan, J-W Cheng and G-Y Yang, *Chemistry – A European Journal*, 2024, **30**, e202400739.
30. J A Konnert, J R Clark and C L Christ, *Am. Mineral.*, 1972, **57**, 381-396.
31. D A Köse, B Zümreoglu-Karan, T Hökelek and E Sahin, *Z. Anorg. Allg. Chem.*, 2009, **635**, 563-566.
32. Z Y Wu, P Branda and Z Lin, *Inorg. Chem.*, 2012, **51**, 3088-3093.
33. T S Ortner, K Wurst, M Seibald, B Joachim and H Huppertz, *Eur. J. Inorg. Chem.*, 2016, **2016**, 3292-3298.
34. Q Wei, S-J Sun, J Zhang and G-Y Yang, *Chemistry – A European Journal*, 2017, **23**, 7614-7620.
35. C-A Chen, W-F Liu and G-Y Yang, *Chem. Commun.*, 2022, **58**, 8718-8721.
36. M Zoller, K Wurst and H Huppertz, 2019, **74**, 757-764.
37. D Neiner, Y V Sevryugina, L S Harrower and D M Schubert, *Inorg. Chem.*, 2017, **56**, 7175-7181.
38. C Jin, X Shi, H Zeng, S Han, Z Chen, Z Yang, M Mutailipu and S Pan, *Angew. Chem. Int. Ed.*, 2021, **60**, 20469-20475.